Electronic supplementary information

The Alloying-Induced Electrical Conductivity of Metal-Chalcogenolate Nanowire

Feng Ke,[a] Chuanjun Zhou,[a] Mengke Zheng,[b] Hao Li,[a] Junjie Bao,[a] Chen Zhu,[a] Yongbo Song,[a] Wen Wu Xu,*[b] and Manzhou Zhu*[a]

[a] Department of Chemistry and Centre for Atomic Engineering of Advanced Materials, Anhui Province Key Laboratory of Chemistry for Inorganic/Organic Hybrid Functionalized Materials, Key Laboratory of Structure and Functional Regulation of Hybrid Materials, Anhui University, Hefei 230601, P. R. China.
[b] Department of Physics, School of Physical Science and Technology, Ningbo University, Ningbo 315211, P. R. China.

Experimental Procedures

Materials and Synthesis

All reagents were used as received without further purification: copper(I) chloride (CuCl, ≥ 99.95%, metals basis)，silver nitrate ($AgNO_3$, ≥ 99%, metals basis), 1-Adamantanethiol ($C_{10}H_{16}S$, ≥ 99%), triphenylphosphine (PPh_3, ≥ 98%), sodium borohydride ($NaBH_4$, ≥ 99.99%), methylene chloride (CH_2Cl_2, HPLC, ≥ 99.9%), acetonitrile (CH_3CN, HPLC, ≥ 99.9%), methanol (CH_3OH, HPLC, ≥ 99.9%), ethanol (CH_3CH_2OH, HPLC, ≥ 99.9%). All reagents were used as received without further purification. All glassware was thoroughly cleaned with aqua regia (HCl : HNO_3 = 3 : 1 vol%), rinsed with copious pure water, and then dried in an oven prior to use.

Synthesis and crystallization of $[Ag_{2.5}Cu_{1.5}(S\text{-}Adm)_4]_n$

Synthesis of the precursors: $AgNO_3$ (50 mg, 0.294 mmol) was dissolved in 200 μL pure water, and 1-Adamantanethiol (100 mg, 0.594 mmol) was dissolved in 15 mL methylene chloride. These two solutions were blended in a 100 mL flask. The solution was vigorously stirred with a magnetic stirring for 30 min and the white haze appeared in the flask. Then, Ph_3P (200 mg, 0.76 mmol. dissolved in 2 mL CH_2Cl_2) were added to the above solution and the white haze become clear quickly. After ~10 min stirring, CuCl (40.0 mg, 0.40 mmol, dissolved in 3 mL CH_3CN) were added to the flask. After ~20 min, the white haze appeared in the solutions, and $NaBH_4$ (60 mg, 1.59 mmol, dissolved in 2 mL ice-cold pure water) were quickly added to the flask. The color of the solution changed from white to black and white haze disappeared. The reaction was allowed to proceed 3 h at room temperature. After removing the aqueous phase, the mixture in the organic phase was dried and washed several times with CH_3OH to remove the redundant 1-Adamantanethiol and byproducts.

Assembly crystallization of nanowires: The NWs were assembled in CH_2Cl_2/C_2H_5OH for 3 – 4 days at room temperature. Single crystals of $[Ag_{2.5}Cu_{1.5}(S\text{-}Adm)_4]_n$ were cultivated by diffusing the ethanol into the methylene chloride solution of precursors. Millimeter scale light brown transparent crystals were collected, and the structure of the MOCs was determined by X-ray crystallography.

Synthesis and crystallization of $[Ag_4(S\text{-}Adm)_4]_n$.

The synthesis of $[Ag_4(S\text{-}Adm)_4]_n$ has been described in previous reports.[1] Briefly, anhydrous $AgNO_3$ and 1-Adamantanethiol were first dissolved in pure water and toluene respectively, at 20 mM concentration. The dissolution of $AgNO_3$ took place at 80 ℃ over a period of 6 h, resulting in a colorless solution. The solutions were then carefully layered in a borosilicate vial with the water phase at the bottom. Crystals nucleated at the interface immediately, and were grow for >72 h at 40 ℃. And the structure of the NWs was demonstrated by PXRD (Fig. S14).

Characterization of electrical conductivity of NWs.

To measure the A.C. impedance of $[Ag_{2.5}Cu_{1.5}(S\text{-}Adm)_4]_n$ and $[Ag_4(S\text{-}Adm)_4]_n$ dry powder samples, ~60 mg dry powders were filled in a cylindrical mold with a diameter of 13.8 mm and pressed into thin sheets. Two stainless steel disks were used as electrodes A.C. impedance spectra were recorded using an impedance analyser (CHI660E, CHI Instruments), with 50 mV peak-to-peak bias voltage in the frequency range of 1 Hz to 1 MHz.[2] The Nyquist plots were fitted with a nonlinear least-square fitting algorithm, implemented in Z-view, and all data points weighted equally.[3] The calculation method of resistivity of NW core is based on the previous report.[2] Through the analysis of the system and the summary of relevant reports,[2] it is found that the resistance behavior of the sample is most suitable for fitting with the equivalent circuit of a capacitor (C1), two resistors (R1 and R2) and a constant-phase element (Q1) (inset in Fig. 3d). C1 and R1 are assigned to the capacitive and resistive behavior of the NW-core, while Q2 and R2 correspond to the resistance of the organic shell coupled with electronic effects from the defects, grain boundaries and contact barriers. And then converting the R1 to NW-core resistivity, NW-core resistivity contribution to the sample resistivity is determined to be 1.07×10^5 Ω·m. The arrangement of NWs powders in the electrochemical cell is random, so the resistivity of the NW-core derived from the sample resistivity must be corrected. In fact, previous studies have shown that this random array of NWs has three orders of magnitude more resistance than directional NWs.

Calculation method of structural relaxations and electronic calculations.

All the structural relaxations and electronic calculations were carried out within the framework of density functional theory (DFT) as implemented in VASP 5.4.[4] Projector-augmented wave[5] potentials and the exchange-correlation interactions formulated within the Perdew−Burke−Ernzerhof generalized gradient approximation (PBE-GGA) were employed.[6] The plane-wave cutoff energy was set to be 500 eV. The van der Waals interactions were included by using DFT-D3 method.[7] All the systems were completely relaxed until the energy and force were converged to 10^{-4} eV and 10^{-2} eV $Å^{-1}$. Vacuum space of 15 Å was adopted to eliminate possible artificial interactions between adjacent NWs.

Instrumentations

Single-crystal X-ray diffraction analyses. Single crystal X-ray diffraction data was collected on a Bruker D8 Venture diffractometer with the Mo K¥α X-ray source (λ = 0.71073 Å). A piece of black plate-shaped crystal with dimensions 0.02 x 0.08 x 0.10 mm was mounted. Data collection was performed at 170 K. Using Olex2, [8] the structure was solved with the ShelXT [9] structure solution program using Intrinsic Phasing and refined with the ShelXL[10] refinement package using Least Squares minimisation. Remaining non-hydrogen atoms were generated via subsequent difference Fourier syntheses. All the non-

hydrogen atoms were refined anisotropically. All the hydrogen atoms were set in geometrically calculated positions and refined isotropically using a riding model. The diffuse electron densities resulting from the residual solvent molecules were removed from the data set using the SQUEEZE routine of PLATON and refined further using the data generated.

UV-visible absorption spectroscopy. The UV-Vis absorption spectrum of the precursors dissolved in DCM were recorded using Agilent 8453 diode array spectrometer. Whose background correction was made using a DCM blank**.**

X-ray photoelectron spectroscopy. X-ray photoelectron spectroscopy (XPS) measurements were performed on Thermo ESCALAB 250 equipped with a monochromated Al Kα (1486.8 eV) 150 W X-ray source, 0.5 mm circular spot size, a flood gun to counter charging effects, and the analysis chamber base pressure lower than 1×10^{-9} mbar; data were collected with FAT = 20 eV.

Thermogravimetric analysis. Thermal gravimetric analysis (TGA) (~15 mg sample used) was conducted in a N_2 atmosphere (flow rate ~ 50 mL/min) on a TG/DTA 6300 analyzer (Seiko Instruments, Inc), and the heating rate was 10 ℃ /min.

Inductively coupled plasma mass spectrometry. Inductively coupled plasma mass spectrometry (ICP-MS) was performed by Thermo iCAP QICP-MS.

Power X-ray diffraction. Powder X-ray diffraction (PXRD) data were collected on a Smart Lab 9 KW with Cu Kα radiation at ambient temperature. The samples used for PXRD tests are $[Ag_{2.5}Cu_{1.5}(S\text{-}Adm)_4]_n$ and $[Ag_4(S\text{-}Adm)_4]_n$ drying crystals power. PXRD measurements were performed at scanning mode of 2Theta/Theta, scanning type of continuous Scanning, incident slit of 1/2deg and receiving slit of 20.00 nm.

Electrochemical Impedance Spectroscopy. Electrochemical Impedance Spectroscopy (EIS) was conducted by a CHI660E electro-chemical workstation (CHI Instruments). Applying a sinusoidal voltage through two stainless-steel disks sandwiching the dry powders. A.C. impedance spectra were recorded with 50 mV peak-to-peak bias voltage, and frequencies were swept from 1 Hz to 1 MHz.

Supplementary Figures.

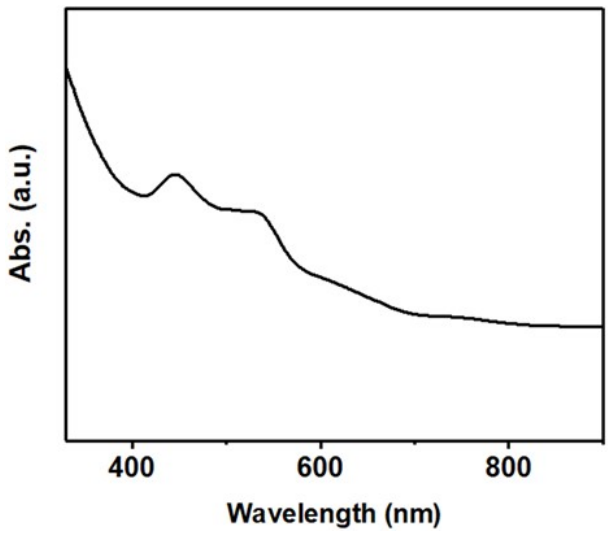

Fig. S1 UV-vis absorption spectrum of the precursors dissolved in DCM solution.

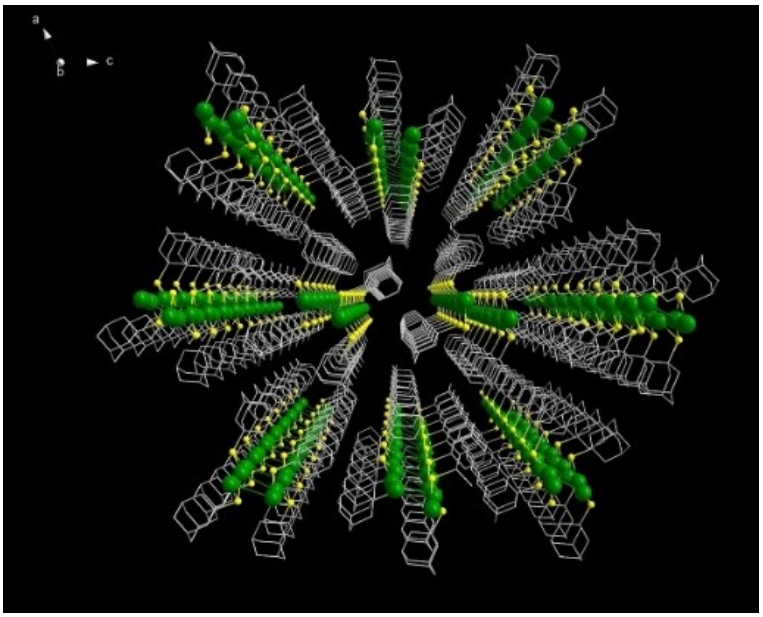

Fig. S2 The view of $[Ag_{2.5}Cu_{1.5}(S\text{-}Adm)_4]_n$ NWs along the b axis. Colour labels: gray = C, orange = S, green = Metal atom. For clarity, all H atoms are not shown, and the adamantane groups are shown in sticks.

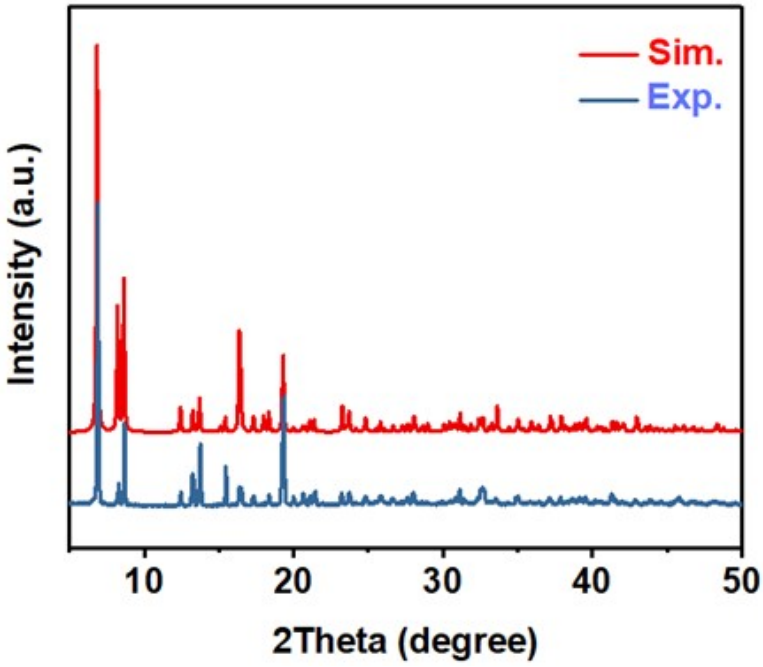

Fig. S3 Comparison of the experimental and theoretical powder X-ray diffraction spectra of $[Ag_{2.5}Cu_{1.5}(S\text{-}Adm)_4]_n$.

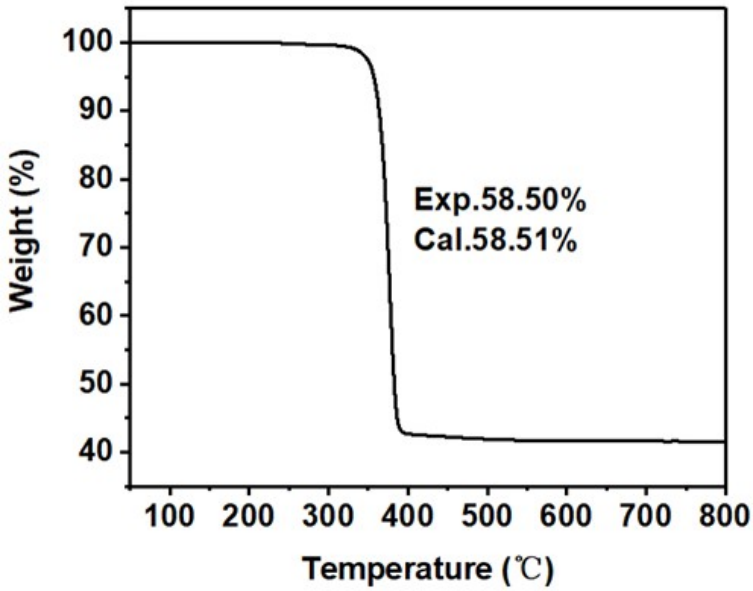

Fig. S4 TGA curve of the $[Ag_{2.5}Cu_{1.5}(S\text{-}Adm)_4]_n$ nanowires. Note: based on their weight loss, the product after calcination was assigned as Cu_2S and AgS_2.

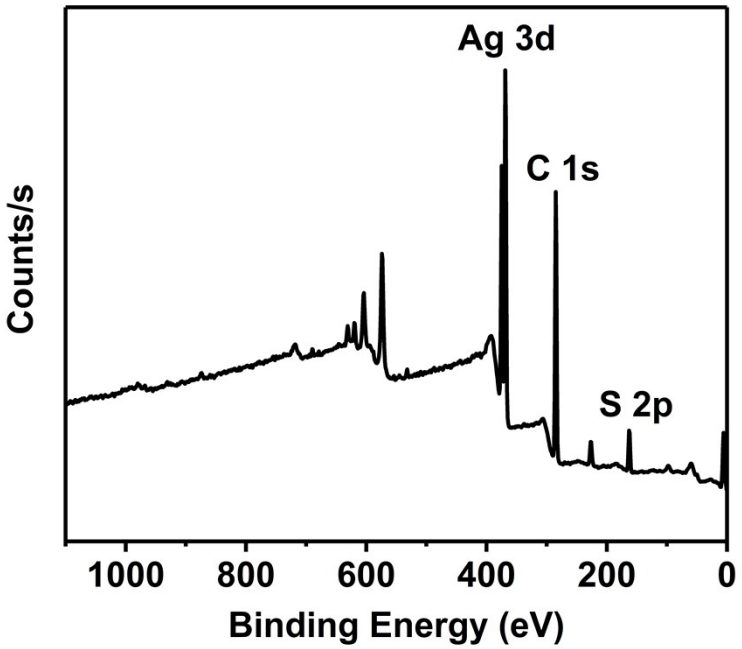

Fig. S5 XPS spectra of the $[Ag_4(S\text{-}Adm)_4]_n$ NWs. The presence of Cu was not found in the spectra.

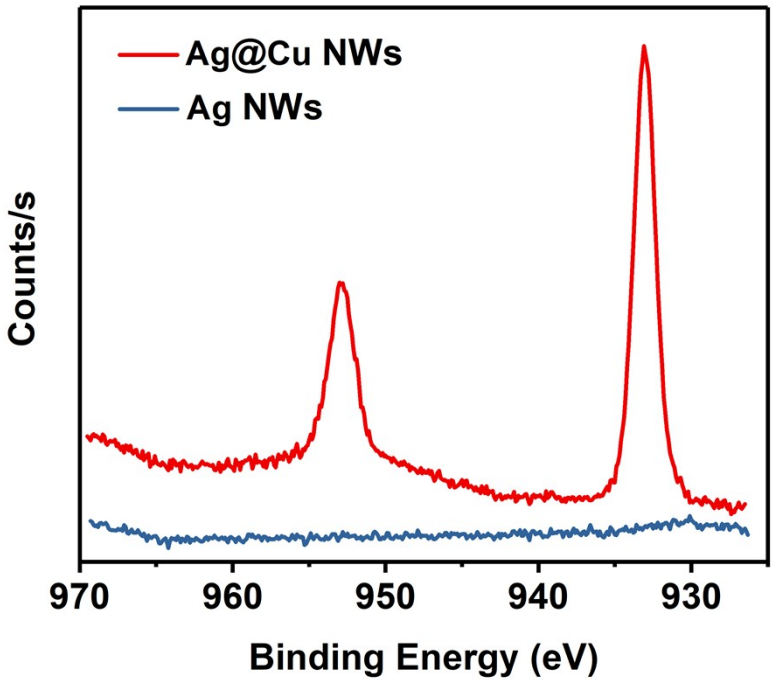

Fig. S6 Comparison of XPS spectrum (Cu 2p) for $[Ag_{2.5}Cu_{1.5}(S\text{-}Adm)_4]_n$ (red) and $[Ag_4(SR)_4]_n$ (blue).

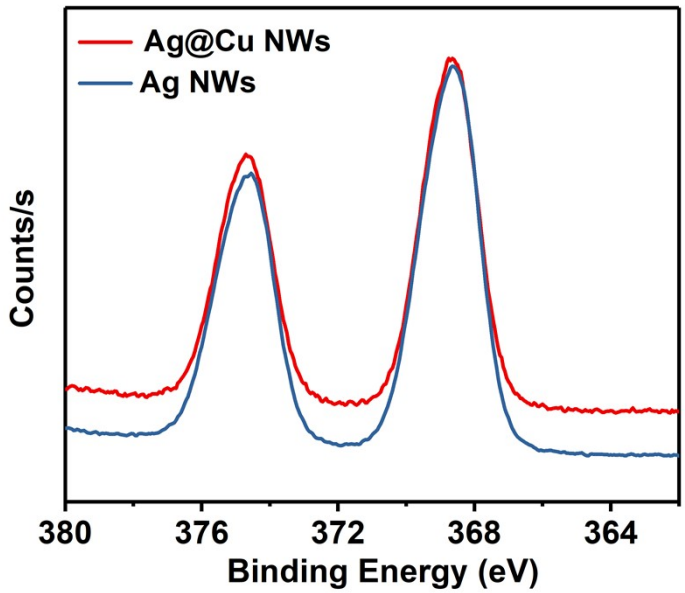

Fig. S7 Comparison of XPS spectrum (Ag 3d) for $[Ag_{2.5}Cu_{1.5}(S\text{-}Adm)_4]_n$ (red) and $[Ag_4(SR)_4]_n$ (blue).

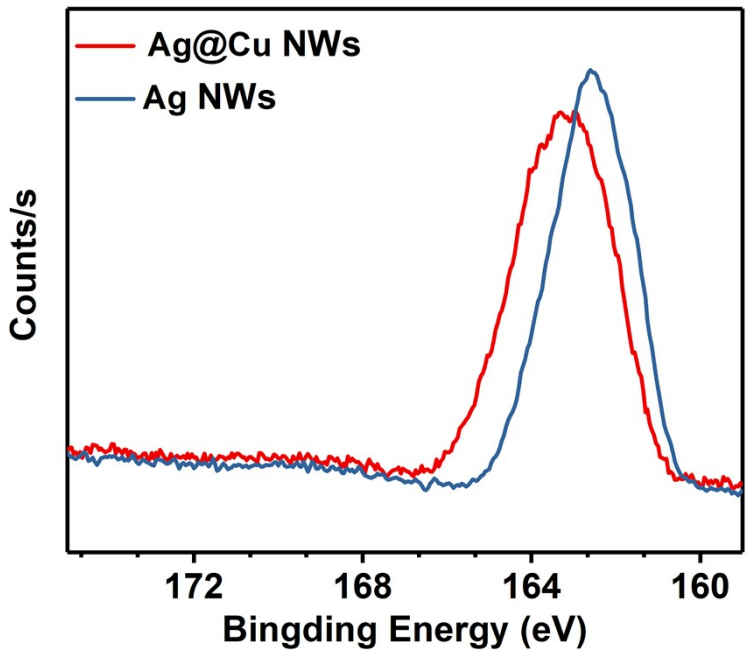

Fig. S8 Comparison of XPS spectrum (S 2p) for $[Ag_{2.5}Cu_{1.5}(S\text{-}Adm)_4]_n$ (red) and $[Ag_4(SR)_4]_n$ (blue).

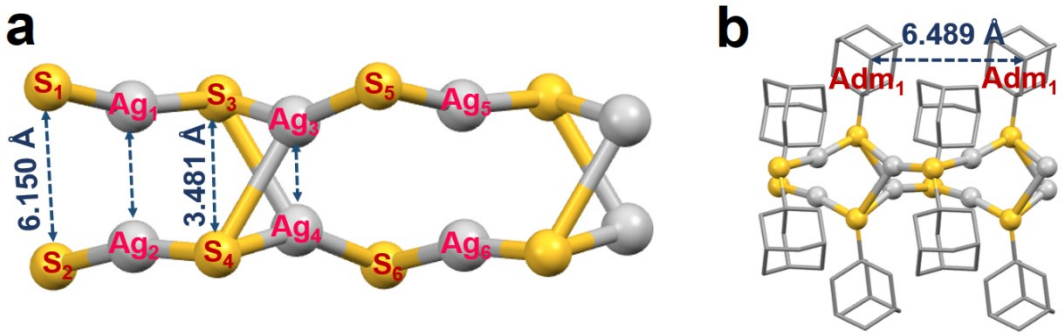

Fig. S9 The structural details and atoms distances of $[Ag_4(S\text{-}Adm)_4]_n$. For clarity, all H atoms are not shown and all C atoms are not shown in a and c. Colour lables: gray = C, orange = S, light gray = Ag, green = Metal atom. Note: The detailed data are shown in Table S2.

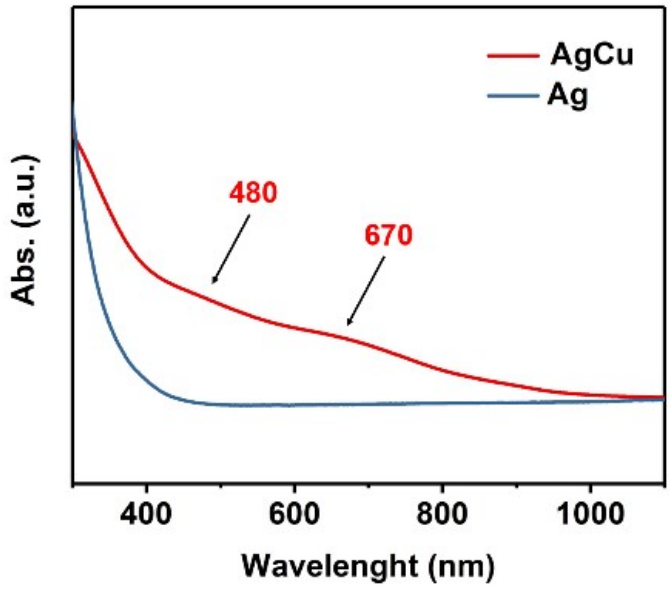

Fig. S10 UV-vis absorption spectra of the crystals of $[Ag_{2.5}Cu_{1.5}(S\text{-}Adm)_4]_n$ (red) and $[Ag_4(SR)_4]_n$ (blue).

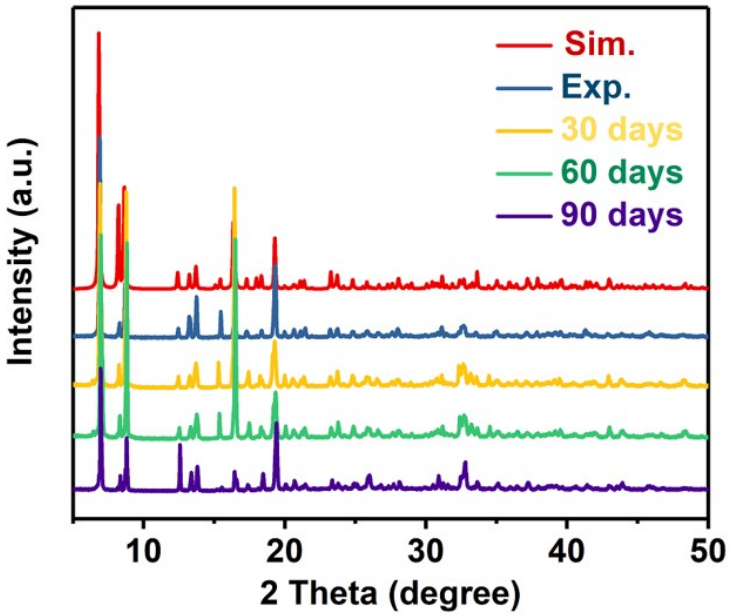

Fig. S11 PXRD spectra of $[Ag_{2.5}Cu_{1.5}(S\text{-}Adm)_4]_n$ in different periods.

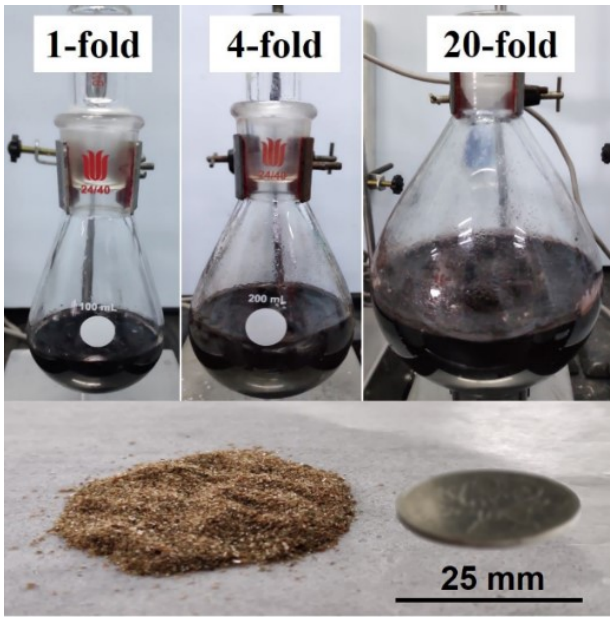

Fig. S12 Photographs of the reactions performed at different scales and the crystals obtained. The scale bar is 25 mm.

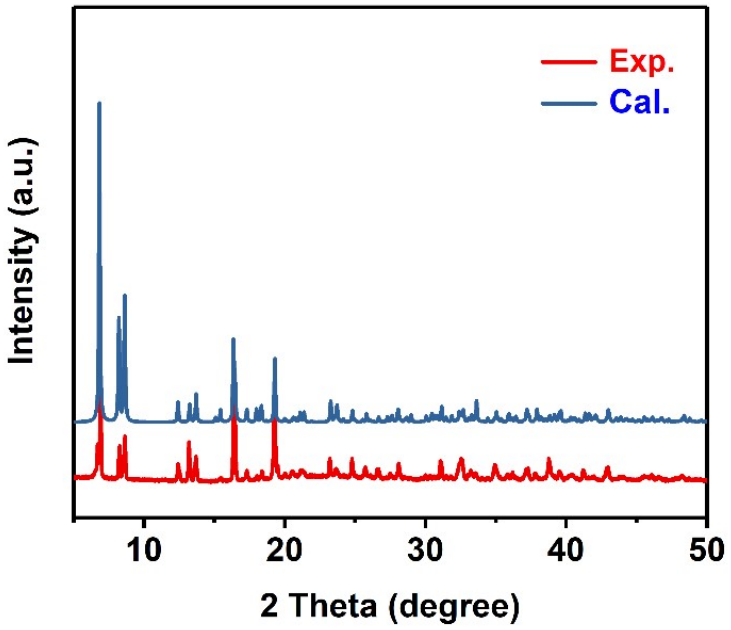

Fig. S13 Comparison of the NW crystals obtained by scaled-up synthesized experimental and theoretical PXRD spectra of $[Ag_{2.5}Cu_{1.5}(S\text{-}Adm)_4]_n$.

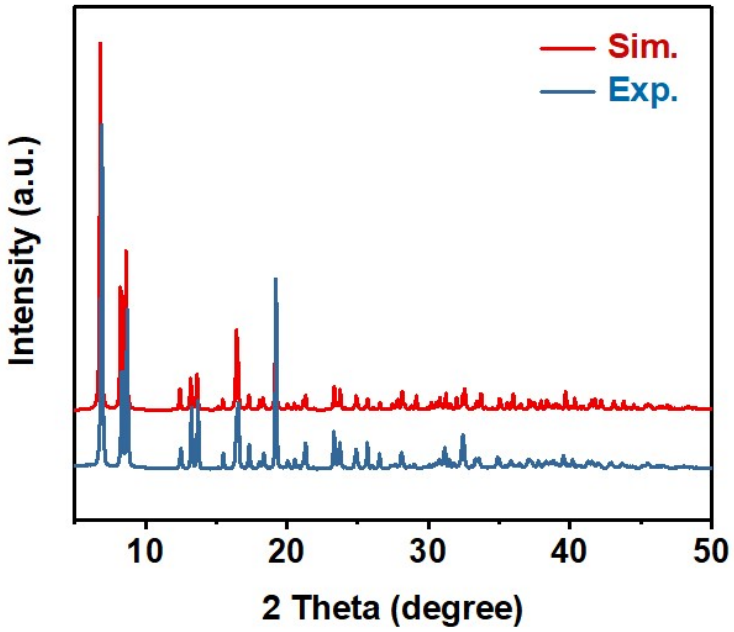

Fig. S14 Comparison of the experimental and theoretical PXRD spectra of $[Ag_4(S\text{-}Adm)_4]_n$ synthesized according to the previous reports. This proves the successful synthesis of silver nanowires.

Supplementary Tables.

Table S1. Comparison of Ag/Cu ratios in different tests.

	SC-XRD	XPS	ICP-MS
Ag : Cu	1.67	1.74	1.70

Table S2. The comparison of bond lengths and group distances between $[Ag_{2.5}Cu_{1.5}(S\text{-}Adm)_4]_n$ and $[Ag_4(S\text{-}Adm)_4]_n$.

	M_1-M_2 (Å) [a]	M_3-M_4 (Å) [b]	S_1-S_2 (Å)	S_3-S_4 (Å)	Adm_1-Adm_2 (Å)	S_1-M_1 (Å)	S_3-M_1 (Å)
Ag@Cu	3.184~2.956	2.815~2.882	5.905	3.439	6.531	2.248	2.409
Ag	3.214	2.923	6.150	3.481	6.589	2.375	2.436

	S_3-M_3 (Å)	S_4-M_5 (Å)	$\angle S_1M_1S_3$ (°)	$\angle M_1S_3M_3$ (°)	$\angle S_3M_3S_5$ (°)	$\angle M_3S_5M_5$ (°)
Ag@Cu	2.349	2.319	166.59	87.30	151.59	91.64
Ag	2.382	2.361	166.89	83.64	150.89	88.81

[a] Each metal atom in $[Ag_{2.5}Cu_{1.5}(S\text{-}Adm)_4]_n$ NWs have a proportion, the distance between M_1 and M_2 is within a range. If both M_1 and M_2 are Cu atoms, the distance is 2.956 Å; if both M_1 and M_2 are Ag atoms, the distance is 3.184 Å. [b] It's the same situation as Table Footnote **a**.

Table S3. The comparison of bond lengths and group distances between DFT-computed structures of NWs doped with different number of copper atoms.

	M_1-M_2 (Å)	M_3-M_4 (Å)	S_1-S_2 (Å)	S_3-S_4 (Å)	Adm_1-Adm_2 (Å)	M-S (Å)
$[Ag_4(SR)_4]_n$	3.237	2.942	6.074	3.817	6.541	2.387
$[Ag_3Cu_1(SR)_4]_n$	3.086	2.791	5.793	3.757	6.527	2.333
$[Ag_2Cu_2(SR)_4]_n$	3.047	2.786	5.599	3.754	6.502	2.277
$[Ag_1Cu_3(SR)_4]_n$	2.776	2.613	5.201	3.699	6.516	2.223
$[Cu_4(SR)_4]_n$	2.629	2.545	4.913	3.631	6.548	2.165

Table S4. Crystal data and structure refinement for $[Ag_{2.5}Cu_{1.5}(S\text{-}Adm)_4]_n$.

Empirical formula	$C_{20}H_{30}Ag_{1.25}Cu_{0.75}S_2$
Formula weight	516.88
Temperature/K	296 (2)
Crystal system	monoclinic
Space group	C2/c
a/Å	29.023(17)
b/Å	6.531(4)
c/Å	23.003(13)
α/°	90
β/°	117.121(6)
γ/°	90
Volume/$Å^3$	3881(4)
Z	8
$\rho_{calc}g/cm^3$	1.769
μ/mm^{-1}	2.298
F(000)	2099.0
Crystal size/mm^3	0.5 ×0.3× 0.2
Radiation	MoKα (λ = 0.71073)
2Θ range for data collection/°	3.154 to 52.048
Index ranges	$-35 \le h \le 35$, $-6 \le k \le 8$, $-26 \le l \le 28$
Reflections collected	13166
Independent reflections	3734 [R_{int} = 0.0553, R_{sigma} = 0.0561]
Data/restraints/parameters	3734/39/236
Goodness-of-fit on F^2	1.048
Final R indexes [I>=2σ (I)]	R_1 = 0.0434, wR_2 = 0.1073
Final R indexes [all data]	R_1 = 0.0752, wR_2 = 0.1206
Largest diff. peak/hole / e $Å^{-3}$	0.92/-0.99

References

1. H. Yan, F. Yang, D. Pan, Y. Lin, J. N. Hohman, D. Solis-Ibarra, F. H. Li, J. E. P. Dahl, R. M. K. Carlson, B. A. Tkachenko, A. A. Fokin, P. R. Schreiner, G. Galli, W. L. Mao, Z. X. Shen, N. A. Melosh, *Nature* **2018**, *554*, 505-510.
2. a) H. Yan, J. N. Hohman, F. H. Li, C. Jia, D. Solis-Ibarra, B. Wu, J. E. Dahl, R. M. Carlson, B. A. Tkachenko, A. A. Fokin, P. R. Schreiner, A. Vailionis, T. R. Kim, T. P. Devereaux, Z. X. Shen, N. A. Melosh, *Nat. Mater.* **2017**, *16*, 349-355. b) Q. Xiao, J. A. Burg, Y. Zhou, H. Yan, C. Wang, Y. Ding, E. Reed, R. D. Miller, R. H. Dauskardt, *Nano Lett.* **2018**, *18*, 4900-4907.
3. T. Okubo, H. Anma, N. Tanaka, K. Himoto, S. Seki, A. Saeki, M. Maekawa, T. Kuroda-Sowa, *Chem. Commun.* **2013**, *49*, 4316-4318.
4. Kresse, G.; Furthmüller, *J. Phys. Rev. B: Condens. Matter Mater. Phys*. **1996**, 54, 11169−11186.
5. Blöchl, P. E. *Phys. Rev. B: Condens. Matter Mater. Phys*. **1994**, 50, 17953−17979.
6. Perdew, J. P.; Burke, K.; Ernzerhof, M. *Phys. Rev. Lett.* **1996**, 77, 3865−3868.
7. Grimme, S.; Antony, J.; Ehrlich, S.; Krieg, H. *J. Chem. Phys*. **2010**,132, No. 154104.
8. Dolomanov, O.V., Bourhis, L.J., Gildea, R.J, Howard, J.A.K. & Puschmann, H. (**2009**), *J. Appl. Cryst.* 42, 339-341.
9. Bourhis, L.J., Dolomanov, O.V., Gildea, R.J., Howard, J.A.K., Puschmann, H. (**2015**). Acta Cryst. A71, 59-75.
10. Sheldrick, G.M. (**2015**). *Acta Cryst*. A71, 3-8.